Hydrodynamic response analysis for a new semi-submersible vessel-shaped fish farm platform based on numerical simulation

Guoliang Pang[1,2], Song Zhang[1], Haiyang Liu[2], Shiyao Zhu[3], Taiping Yuan[1,2], Gen Li[1,2], Xiangxi Han[4] and Xiaohua Huang[1,2]*

[1]Key Laboratory of Open-Sea Fishery Development, South China Sea Fisheries Research Institute, Chinese Academy of Fishery Science, Ministry of Agriculture and Rural Affairs, Guangzhou, China, [2]Key Laboratory of Efficient Utilization and Processing of Marine Fishery Resources of Hainan Province, Sanya Tropical Fisheries Research Institute, Sanya, China, [3]School of Engineering and Information Technology, University of New South Wales, Canberra, NSW, Australia, [4]Key Laboratory of Beibu Gulf Offshore Engineering Equipment and Technology, Education Department of Guangxi Zhuang Autonomous Region, Beibu Gulf University, Qinzhou, China

Due to polluted environments, limited resources, and restricted space in coastal aquaculture, the use of a large-scale aquaculture platform in deep-sea areas has become more important in fish farming. However, the environment in the deep sea is complex and harsh, which threatens the safety of the fish farm platform due to extreme weather. In this work, we developed a new semi-submersible vessel-shaped truss fish farm platform with single-point mooring, considering different operating conditions. The dynamic performance of the platform was analyzed numerically. Firstly, a numerical model of the fish farm platform was created. A physical model test was then executed to verify the numerical model. The results from the numerical model were found to be in good agreement with the experimental results. Subsequently, the dynamic response of the platform under different wave conditions was analyzed based on the validated numerical model. The results showed that the new semi-submersible vessel-shaped fish farm platform had good adaptability to extreme sea conditions. The experimental and numerical analyses of the hydrodynamic responses of the fish farm platform facilitated the design, analysis, and application of the large deep-sea fish farm platform.

KEYWORDS

vessel-shaped fish farm platform, SPM, Hydrodynamic response, mooring tension, numerical simulation

1 Introduction

With population growth, economic progress, and rapid urbanization, the demand for food has increased exponentially. As an indispensable part of the human diet, fish is not only a source of high-quality protein but is also key to ensuring food security in the future. Owing to traditional marine fisheries having been fully developed or overexploited,

mariculture is playing an important role in meeting the demand for fish (Chu et al., 2020). Mariculture can be classified into coastal, off-the-coast, and deep-sea types. In recent years, problems such as the degradation of water quality, the frequent occurrence of biological diseases, and environmental pollution have existed in coastal and off-the-coast mariculture areas, which have directly hindered the sustainable development of the mariculture industry. Therefore, research on deep-sea mariculture based on a large-scale fish farm platform has become more and more important worldwide (Xu and Qin, 2020).

Traditional high-density polyethylene (HDPE) net cages have been commonly used, and analysis of the corresponding hydrodynamic responses has been widely performed using numerical and experimental methods (Fredriksson et al., 2003; Fredriksson et al., 2007; Zhao et al., 2007; Kristiansen and Faltinsen, 2012; Kristiansen and Faltinsen, 2015; Huang et al., 2016; Gansel et al., 2018; Huang et al., 2018). However, the environment in the deep sea is extremely complex and harsh. As a result, the large steel fish farm platform is becoming the one of available facilities for developing deep-sea aquaculture and various forms of large steel fish farm platforms have been being developed intensely developed, and the large steel fish farm platform is one of the available facilities for developing deep-sea aquaculture. A lot of experimental and numerical studies on the hydrodynamic characteristics of these fish farm platforms have also been carried out. Rui (2018) established the finite element model (FEM) of "Ocean Farm 1" based on SESAM and analyzed the hydrodynamic properties of the platform under different wave conditions. It was found that the influence of the cage net on the amplitude of the motion of the platform was not large, but the effect on the mean position of the body cannot be neglected. Zhao et al. (2019) carried out a physical model test of a fish farm platform similar to "Ocean Farm 1" and analyzed the motion and mooring characteristics of the platform under different draught conditions. In addition, Liu et al. (2020, 2021) utilized a numerical simulation method to study the hydrodynamic characteristics of a platform in waves and uniform currents. Moreover, in order to understand the flow field characteristics of a fish farm platform under waves and currents, computational fluid dynamics (CFD) was used by a number of researchers instead of the classical potential flow theory (Martin et al., 2020; Wang et al., 2021; Wang et al., 2022). Li et al. (2018a, 2018b, 2019) presented a vessel-shaped offshore fish farm and conducted a systematic study on the coupled dynamic response and optimization of the mooring lines. In addition, to improve the rate of sea utilization, Lei et al. (2020, 2021) presented a novel offshore floating wind turbine integrated with a steel fish farming cage. With regard to the structural security of the fish farm platform, Yu et al. (2019) studied the local and global responses of an offshore fish farm subjected to ship impacts, while Wang et al. (2020) gave a set of test methods for evaluating the fatigue strength of a copper alloy netting structure. Previous studies indicate that the development of deep-sea mariculture was the consensus in the industry. However, there was no agreement on the types of facilities suitable for this activity. Thus, corresponding studies on types of fish farm platforms have been conducted all over the world. Still, one thing is clear: a fish farm platform with excellent hydrodynamic performance is necessary to develop deep-sea mariculture.

The "DEHAI 1" fish farm platform (Figure 1A) is a semi-submersible vessel-shaped truss platform with single-point mooring (SPM) developed in 2018 by the South China Sea Fisheries Research Institute, Chinese Academy of Fishery Sciences (Huang et al., 2020). This platform successfully resisted the attack of super typhoon Mangkhut in 2018 (Figure 1B), making it the first fish farm platform in the world to "pass the test" against a grade 17 super typhoon. Following that, similar fish farm platforms with different cultured water volumes were designed and stationed in Hong Kong and Hainan, China. However, it should be noted that the current DEHAI series fish farm platforms are all arranged in sheltered sea areas close to the shore and that the operating water depths are all less than 20 m.

To develop deep-sea mariculture and cope with the harsh environment in deep-sea areas, a new semi-submersible vessel-

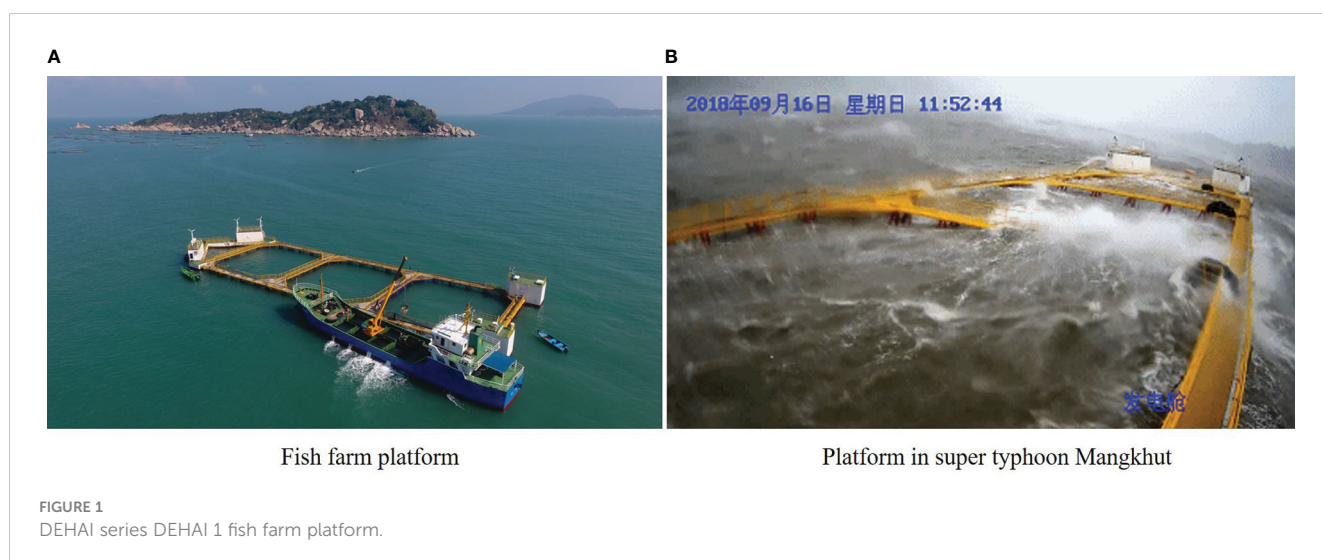Fish farm platform

Platform in super typhoon Mangkhut

FIGURE 1
DEHAI series DEHAI 1 fish farm platform.

shaped fish farm platform with SPM was presented based on technological accumulation from the DEHAI series fish farm platforms. There are structural differences between the new fish farm platform and the current DEHAI series platforms. These are described in detail in a subsequent section. For this new fish farm platform, the hydrodynamic characteristics need to be analyzed. This paper is organized as follows. The numerical model of the fish farm platform is established in *Section 2*. The physical model test and the verification of the numerical model of the fish farm platform are presented in *Section 3*. An analysis of the hydrodynamic characteristics of the platform based on the verified model is presented in *Section 4*. The applicability of the new fish farm platform to deal with extreme sea conditions, which was evaluated through the aspects of motion response and mooring line tension, is discussed in *Section 5*. Finally, the conclusions of this research are presented in *Section 6*.

2 Numerical model establishment

2.1 Fish farm platform parameters

The diagram of the developed semi-submersible vessel-shaped fish farm platform and the definition of the coordinate system are shown in Figure 2. This platform mainly consisted of a steel tube truss, pontoons in the bow and stern, a baffle, and a mooring system. The net was tied to the adjacent truss steel tubes to form three cultured spaces. The baffle in the bow was used to resist the current. The ballast tanks are located at the bottom of the pontoons. The new fish farm platform and the current DEHAI series platforms mainly differed in terms of pontoon type. The pontoons of the new platform had a small waterplane area, and the platform can have different draughts by adjusting the ballast. Figure 3A shows the two draught conditions of the fish farm platform: normal condition and survival condition. In most cases, the platform was in normal condition for aquaculture production. During extreme weather, the platform will dive the main body

through the water. This is referred to as the survival condition in this paper. Due to the pontoons being built with a small waterplane area, the wave and current load acting on the fish farm platform under the survival condition would be reduced, which could help in coping with extreme ocean environments.

A "Y"-type SPM system has been used in the new fish farm platform. Two mooring lines come out of the fairleads of the pontoons in the bow, and these two lines converge at one point into one line. A steel clump weight was arranged at the convergence point, with the end of the mooring line serving as an anchor. Figure 3B shows the diagram of the vertical and lateral views of the fish farm platform. From the figure, the "Y"-type SPM in vertical view can be clearly seen. Due to the weathercock effect from the SPM, the fish farm platform will be moored at the position with the least environmental force. In addition, the platform rotates around the mooring point, which will increase the diffusion space of waste and excreta in the aquaculture area to ensure the quality of the aquaculture water.

The main structure of the fish farm platform is 102.2 m long, 35.1 m wide, and 9 m high. The cultured water volume is nearly 20,000 m^3. The main parameters of the fish farm platform are shown in Table 1.

2.2 Numerical tool and hydrodynamic theory

An analysis of the hydrodynamic responses of the new semi-submersible vessel-shaped fish farm platform was implemented based on the hydrodynamic software AQWA (ANSYS, 2018). According to the structural characteristics of the platform, two types of elements were used in the simulation. The baffle and pontoons in the bow and stern were simulated using a panel method based on potential flow theory. For the steel tube truss system, the Morison equation was used to calculate the wave force of the steel tubes.
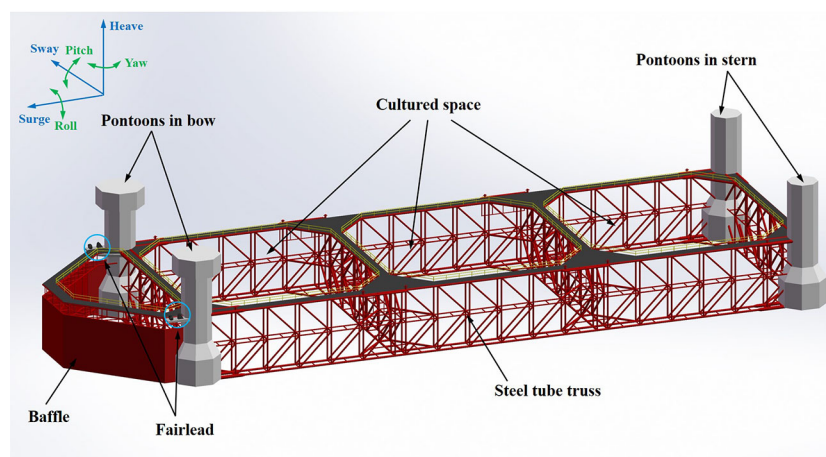

FIGURE 2
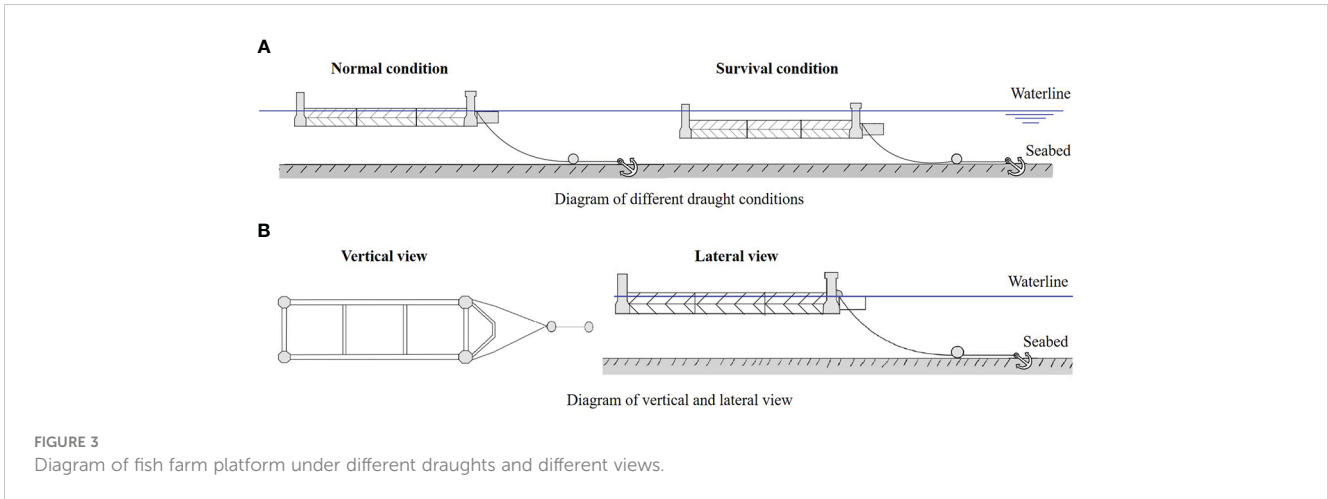Diagram of the new semi-submersible vessel-shape fish farm platform.

FIGURE 3

Diagram of fish farm platform under different draughts and different views.

TABLE 1 Fish farm platform parameters.

Component	Parameter	Value
Main body of platform	Length (m)	102.2
	Width (m)	35.1
	Height (m)	9
	Draught in normal condition (m)	8.2
	Draught in survival condition (m)	14
	Operating water depth (m)	30
Pontoons	Height of pontoons in the bow (m)	17.5
	Height of pontoons in the stern (m)	17.0
	Shape	Eight prism
Mooring steel chain	Length (m)	90
	Weight per meter (kg/m)	84.12
	Fracture force (N)	2,940,000

The floating body's dynamic equation under different environmental loads can be expressed as:

$$(M + \Delta M)\ddot{X} + (B_{\mathbf{rad}} + B_{\mathbf{vis}})\dot{X} + (K_{\mathbf{sw}} + K_{\mathbf{m}})X$$

$$= F_1 + F_{2\mathbf{low}} + F_{2\mathbf{high}} + F_{\mathbf{w}} + F_{\mathbf{c}} + F_{\mathbf{other}} \quad (1)$$

where M is the mass matrix of the floating body; ΔM is the added mass matrix; B_{rad} and B_{vis} are the radiation and viscous damping matrices, respectively; K_{sw} is the stiffness matrix of still water; and K_{m} is the mooring stiffness matrix. F_1 is the first-order wave frequency load; $F_{2\mathrm{low}}$ is the second-order low-frequency load; $F_{2\mathrm{high}}$ is the second-order high-frequency load; F_{w} is the wind load; F_{c} is the current load; and F_{other} denotes other loads.

The flow field was assumed to be inviscid, irrotational, and incompressible. The fluid motion can be described using the three-dimensional (3D) potential flow theory. There is unsteady velocity potential, Φ, in the flow field, which can be classified into either incident

potential, Φ_{I}; diffraction potential, Φ_{D}; or radiation potential, Φ_{R}.

$$\Phi = \Phi_{\mathbf{I}} + \Phi_{\mathbf{D}} + \Phi_{\mathbf{R}} \quad (2)$$

The Φ_{I} variable is known, while Φ_{D} and Φ_{R} can be obtained using corresponding methods. With a known velocity potential, Φ, the pressure distribution of the flow field can be calculated to obtain the overall fluid force acting on the floating body.

The Morison equation is usually employed to calculate the fluid forces acting on the cross-section of a slender structure, and it can be expressed as:

$$dF = \frac{1}{2}\rho D C_{\mathbf{d}}|u_{\mathbf{f}} - u_{\mathbf{s}}|(u_{\mathbf{f}} - u_{\mathbf{s}}) + \rho A C_{\mathbf{m}}\dot{u}_{\mathbf{f}} - \rho A(C_{\mathbf{m}} - 1)\dot{u}_{\mathbf{s}} \quad (3)$$

where C_{d} is the drag coefficient; D is the characteristic drag diameter; u_{f} is the transverse directional fluid particle velocity; u_{s} is the transverse directional structure velocity; C_{m} is the inertia coefficient; $C_{\mathrm{a}}(C_{\mathrm{a}} = C_{\mathrm{m}} - 1)$ is the added mass coefficient; and A is the cross-sectional area.

2.3 Fish farm platform model

The geometric model of the fish farm platform was created using the DM module in ANSYS Workbench. The surface bodies were used to simulate the baffle and the pontoons, while the truss system of the platform was simulated by the line bodies. The geometric model of the fish farm platform is shown in Figure 4A.

The geometric model was then imported into the AQWA module. Considering mesh convergence and computational efficiency, the maximum element size was set to 0.5 m, and the automatic meshing technology in AQWA was used to generate the mesh. The FEM of the fish farm platform (Figure 4B) had 32,219 elements in total. The floating and diving of the fish farm platform are achieved by adjusting the ballast water of the pontoon, with the ballast water being simulated by the mass point in AQWA. The corresponding ballast water parameters under normal operating and extreme survival conditions are shown in Tables 2, 3. After the mooring lines were arranged, the final numerical model of the fish farm platform was updated, as shown in Figure 5.

FIGURE 4
Model of fish farm platform.

FIGURE 5
Model of fish farm platform with mooring lines.

FIGURE 6
Physical model of fish farm platform.
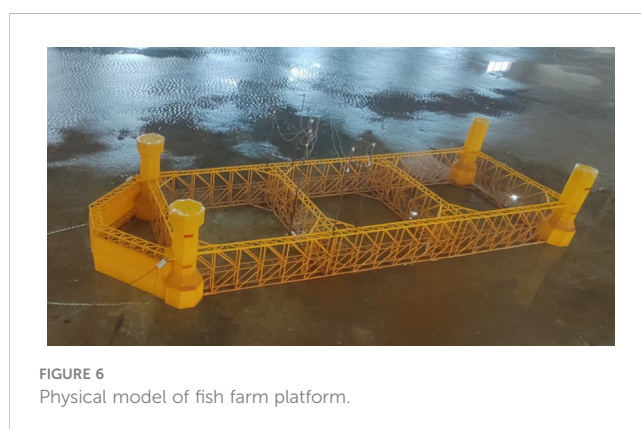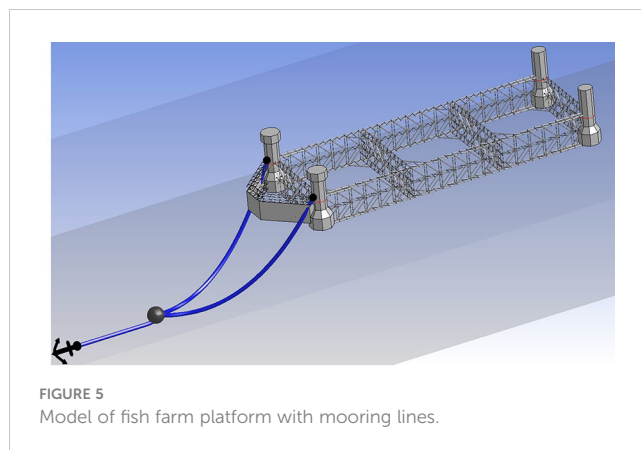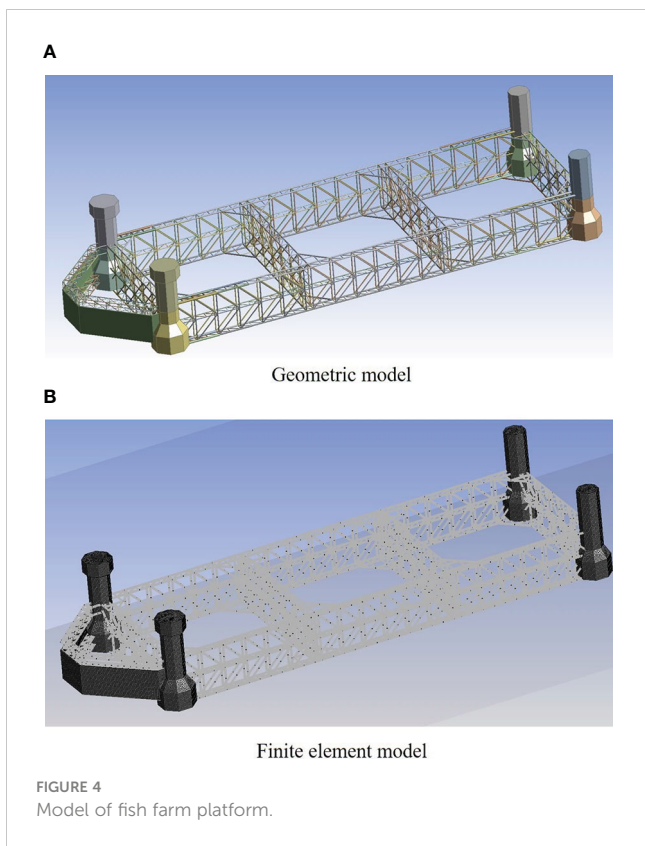
3 Model verification

3.1 Physical model test

In order to validate the numerical model of the fish farm platform, a physical model test was conducted at the Rudong Test Base of the China Academy of Fishery Sciences. Considering the actual platform size, wave tank conditions, and the model cost, among other factors, the model scale was set to 1:40. The physical model of the fish farm platform is shown in Figure 6.

Figure 7 shows the physical model test site condition. The measuring point was fixed to the platform, and the platform's 6 DOF (degrees of freedom) motion was measured using the 3D motion capture system. A wave height gauge and a flow meter were arranged to monitor the wave height and flow velocity, respectively. Strain-type tension gauges were adopted to measure the mooring line tension. The maximum tension from the tension gauges was recorded,

TABLE 2 Ballast water parameters under normal operating conditions.

Draught 8.2 m	Mass (kg)	I_{xx} (kg·m^2)	I_{yy} (kg·m^2)	I_{zz} (kg·m^2)
Ballast water in the bow (left)	128,690.3471	438,075	438,075	677,935
Ballast water in the bow (right)	128,690.3471	438,075	438,075	677,935
Ballast water in the stern (left)	106,316.7612	423,223	423,223	558,458
Ballast water in the stern (right)	106,316.7612	423,223	423,223	558,458

TABLE 3 Ballast water parameters under extreme survival conditions.

Draught 14 m	Mass (kg)	I_{xx} (kg·m^2)	I_{yy} (kg·m^2)	I_{zz} (kg·m^2)
Ballast water in the bow (left)	208,619.73	1,310,000	1,310,000	1,000,000
Ballast water in the bow (right)	208,619.73	1,310,000	1,310,000	1,000,000
Ballast water in the stern (left)	204,827.52	1,970,000	1,970,000	766,860.69
Ballast water in the stern (right)	204,827.52	1,970,000	1,970,000	766,860.69

FIGURE 7
Physical modeling test site condition.
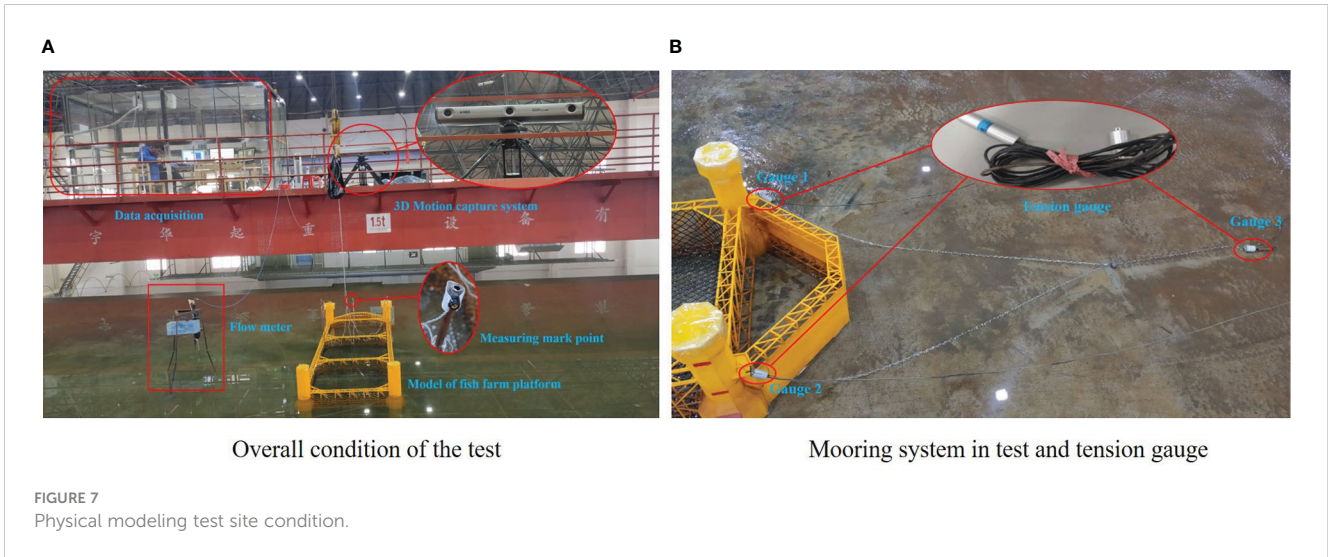
which usually occurred at gauge 1 or gauge 2 (Figure 7). Because of symmetry, the two tensions from gauges 1 and 2 were almost the same.

3.2 Motion response and mooring line tension comparison

Three regular wave conditions (H = 5 m, T = 9 s; H = 6 m, T = 11 s; and H = 7 m, T = 13 s) were selected for comparative verification. The results showed that the motion response values in

roll, sway, and yaw were small due to the adoption of the Y-type SPM. Thus, only the motion responses in the heave and pitch of the physical model test and the numerical simulation were compared, as shown in Figure 8. It was noted that the numerical simulation curves showed good agreement with the physical model test curves. Figure 9 shows the maximum mooring line tension of the physical model test and the numerical simulation under different wave conditions. The maximum error occurred in the H = 7 m, T = 13 s wave condition, with a value of 4.35%. The comparison of the motion response and mooring line tension between the

FIGURE 8
Comparison of motion responses between physical model test and numerical simulation under different wave conditions.
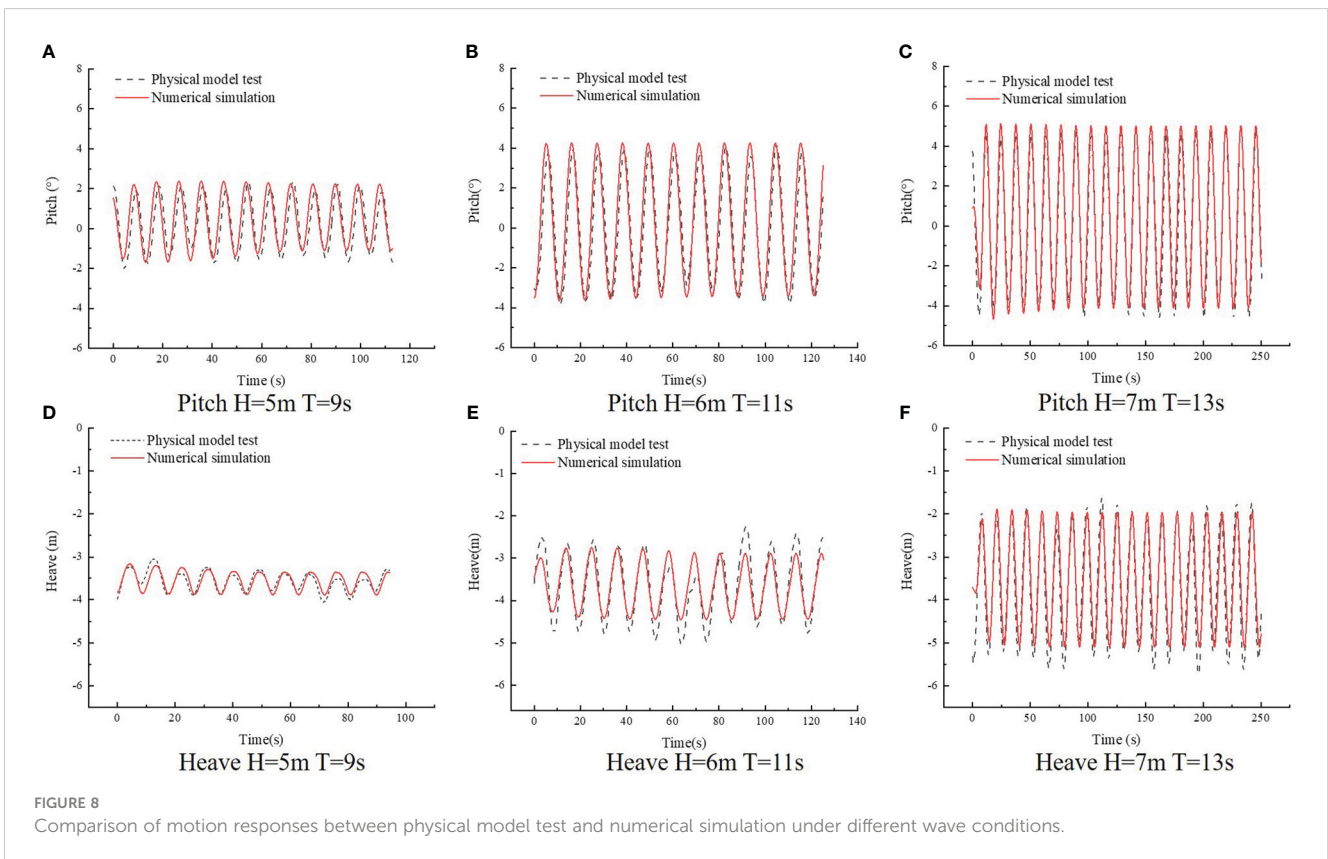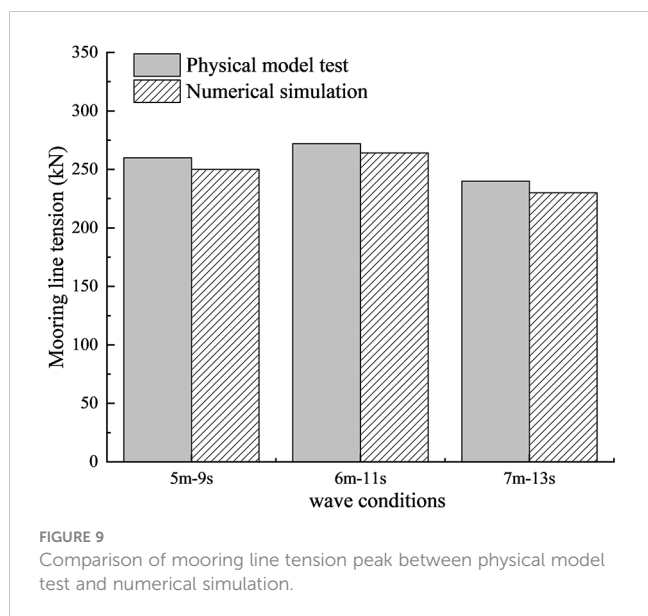
FIGURE 9
Comparison of mooring line tension peak between physical model test and numerical simulation.

physical model test and the numerical simulation demonstrated the effectiveness of the numerical model of the fish farm platform and the corresponding modeling method.

4 Motion response and mooring characteristic analysis

4.1 Motion response

To study the response characteristics of the fish farm platform with different wave parameter changes, the platform's motion response and mooring characteristics were analyzed under a

series of regular waves. Nine groups of wave conditions were considered, with wave heights from 6 to 10 m and wave periods from 9 to 13 s. The wave conditions are shown in Table 4. It should be noted that, as the platform was in normal condition most of the time, only the draught of 8.2 m was considered. In addition, for this type of SPM vessel-shaped platform, the motion responses in roll, sway, and yaw were very small; thus, only the motion responses in pitch, heave, and surge were analyzed.

Figure 10 shows the motion response of the fish farm platform under different wave conditions. It was found that the motion response was positively correlated with the wave height and wave period in the pitch and heave motions. When the wave height increased from 6 to 10 m, the average amplitude increases were 41.47%, 21.89%, and 41.50%, respectively, corresponding to the pitch motion under wave periods of 9, 11, and 13 s, respectively. In addition, when the wave period increased from 9 to 13 s, the average amplitude increases of the pitch motion under wave heights of 6, 8, and 10 m were 138.27%, 137.77%, and 138.33%, respectively. These indicate that the pitch motion was more sensitive to the change of wave period than of wave height. Similar results were obtained for the heave motion, as shown in Figure 10B, which also illustrates the correlation between the pitch and heave motions. The difference was that, under the condition of a large wave period, the heave motion increased more obviously with increasing wave height. Similarly, surge motion also increased with the increase in wave height, but there was no obvious correlation with the change in wave period.

4.2 Mooring line tension and laid length

The mooring line tension values of the fish farm platform under different wave conditions are shown in Figure 11. It was observed

TABLE 4 Different wave conditions.

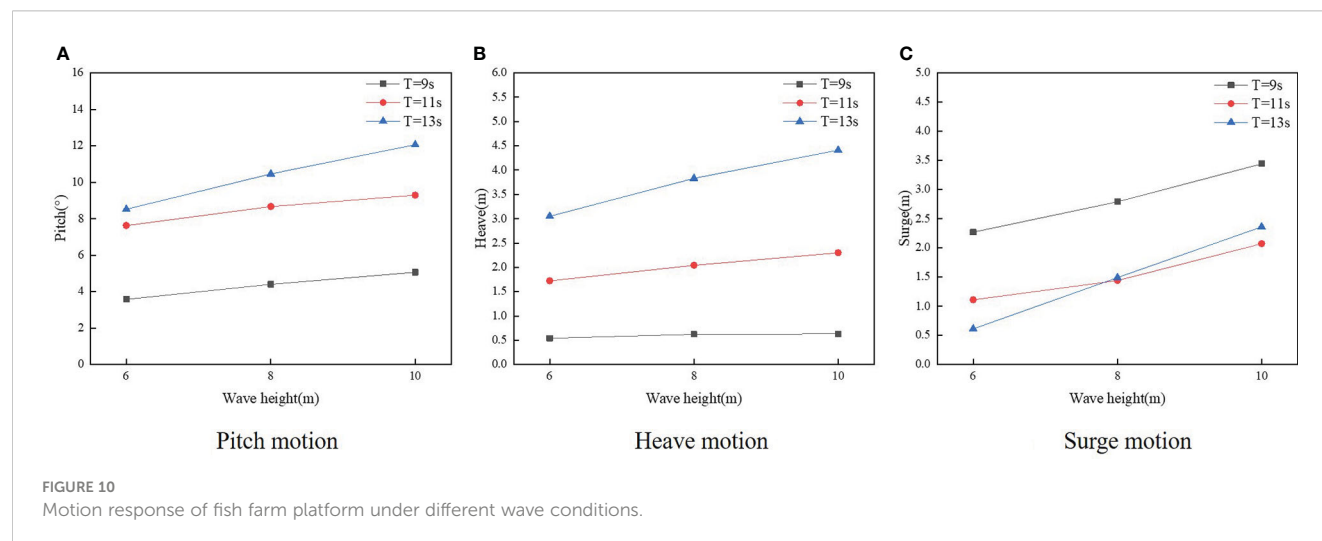| Conditions	1	2	3	4	5	6	7	8	9
Wave height (m)	6	8	10	6	8	10	6	8	10
Wave period (s)	9	9	9	11	11	11	13	13	13

FIGURE 10
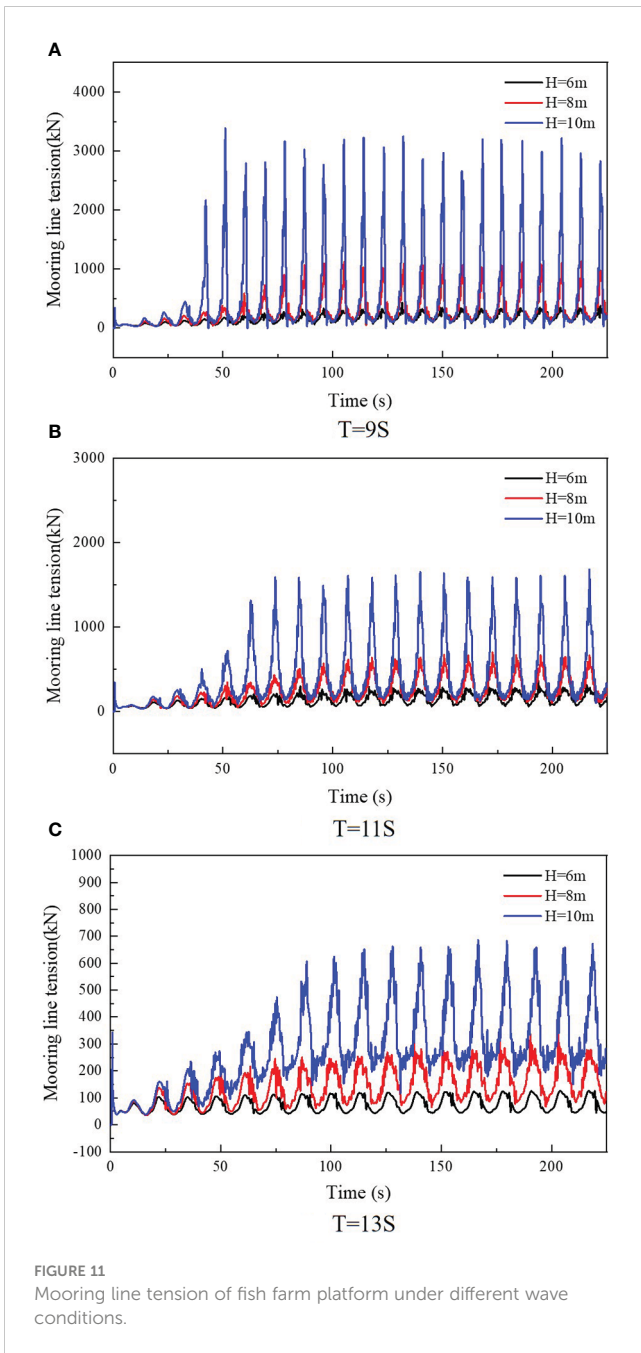Motion response of fish farm platform under different wave conditions.

FIGURE 11
Mooring line tension of fish farm platform under different wave conditions.
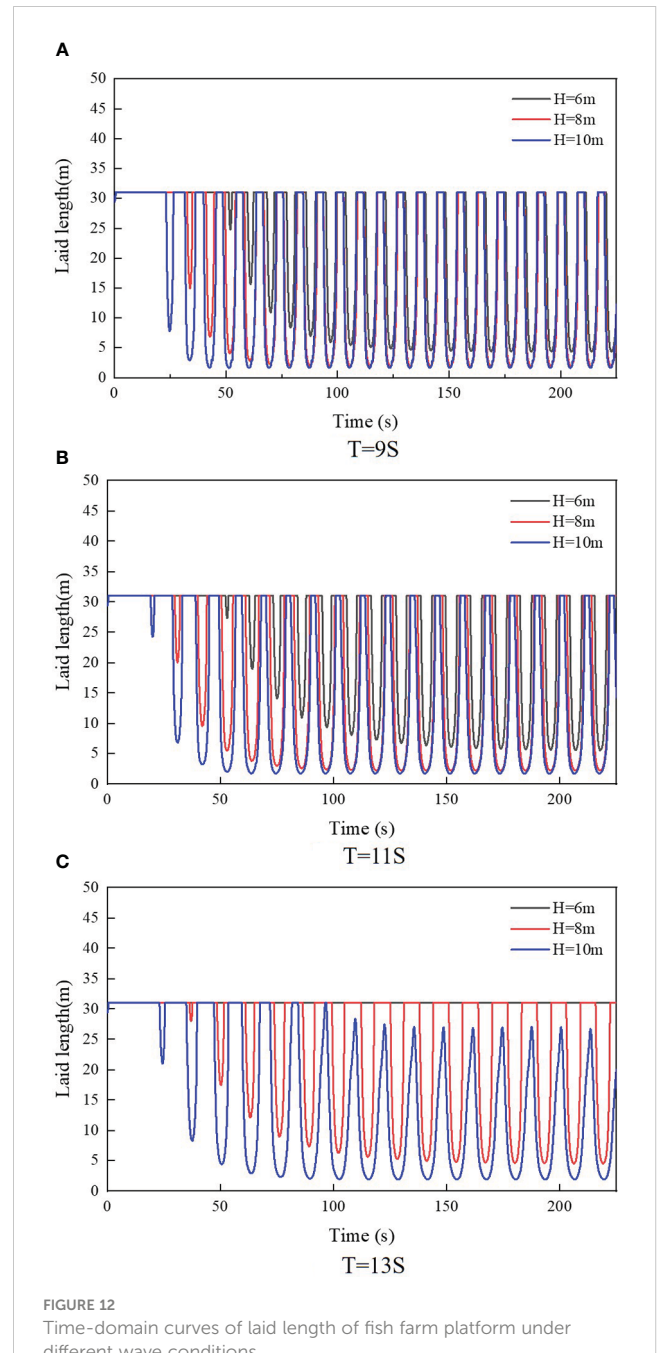

FIGURE 12
Time-domain curves of laid length of fish farm platform under different wave conditions.

that the mooring line tension was positively correlated with the wave height and negatively correlated with the wave period. Compared with the condition of small wave height, especially under the condition of large wave height, the mooring line tension increased more with the decrease of wave period.

Figure 12 shows the laid length of the fish farm platform under different wave heights. It was found that the minimum laid length was negatively correlated with the wave height; that is, the higher the wave height, the shorter the minimum laid length. A comparison of the laid length of the fish farm platform under different wave periods found that the minimum laid length was positively correlated with the wave period; that is, the longer the wave period, the greater the minimum laid length. A close check of Figures 11, 12 revealed a correlation between laid length and

mooring line tension. A high mooring line tension corresponded to a short laid length, and with a large laid length, the mooring line tension would be low. It was concluded that, in addition to the mooring line tension of the fish farm platform, the laid length of the mooring line is also a key factor in judging mooring safety. A long laid length not only can ensure the anchor's bottom grasping ability but also plays a buffer role under the dynamic load transmitted by the connected platform.

To further understand the hydrodynamic characteristics of the fish farm platform under different wave conditions, the wave steepness parameter was adopted. Nine wave steepness independent variables were calculated, as shown in Table 4. The motion response and mooring line tension of a fish farm platform

were obtained and illustrated in Figures 10, 12. The motion response and the mooring line tension of the fish farm platform under different wave steepness conditions are shown in Figure 13.

It can be seen that the pitch and heave motions showed consistent change characteristics with the increase of wave steepness, proving the correlation between these two motions. In addition, the overall change trends of the surge motion and mooring tension significantly increased with the increase of wave steepness. This indicates that surge motion played an important role in the increase of the mooring force. Moreover, attention should be paid to waves with high steepness values when designing a mooring system.
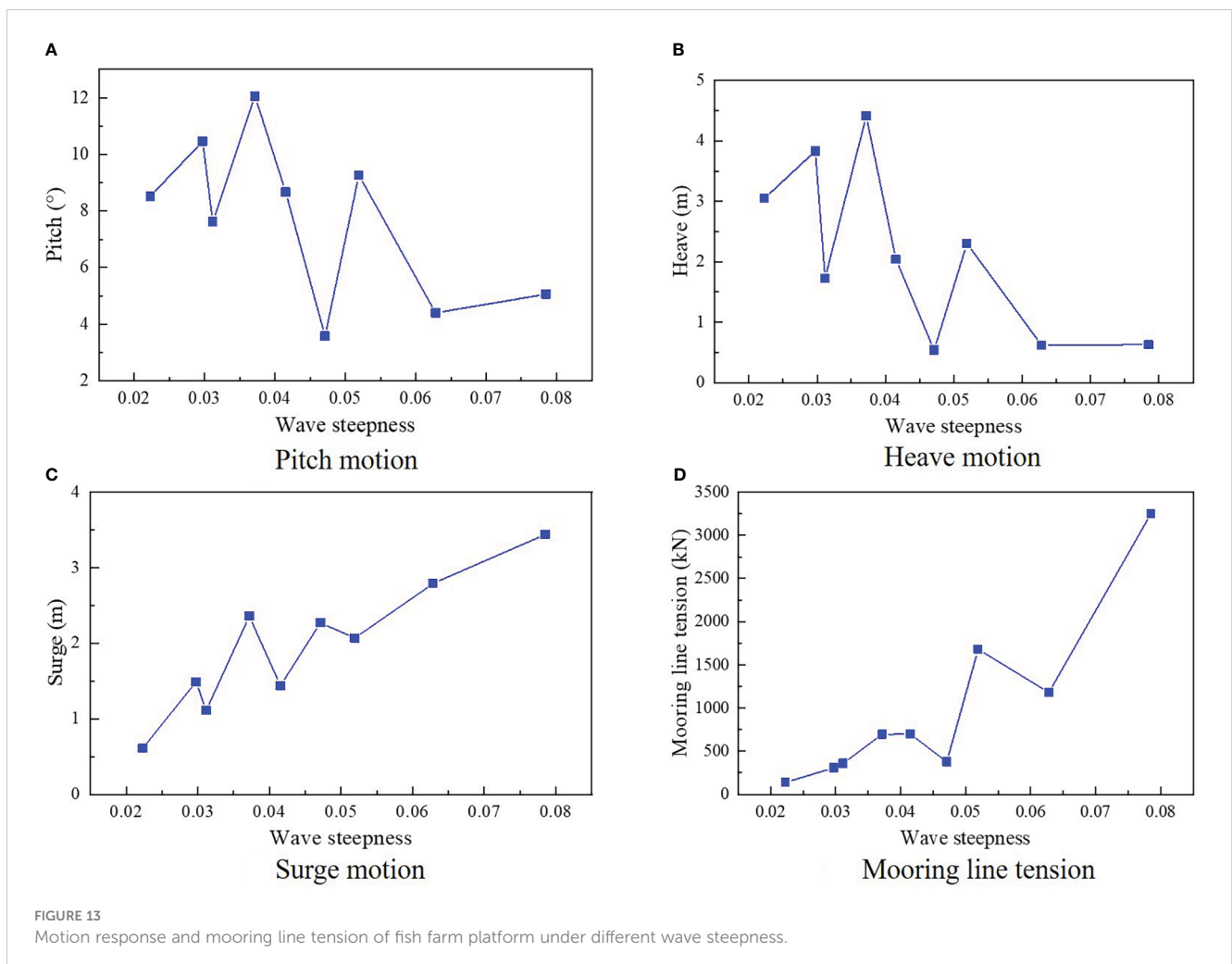
5 Applicability of the platform to deal with extreme sea conditions

5.1 Motion response

The new semi-submersible vessel-shaped fish farm platform in this study was designed to deal with extreme ocean conditions by diving the main body of the platform through the water. To evaluate

the applicability of the platform in extreme sea conditions, its hydrodynamic characteristics under diving conditions were analyzed and compared with those under normal operating conditions. The same wave conditions were considered, as listed in Table 4.

Figure 14 shows the motion response comparison of the fish farm platform under the normal condition and the survival condition. It was observed that, with the increase in the draught, the motion response of the platform decreased to varying degrees. In detail, the pitch motion under the survival condition was smaller than that under the normal condition, but the range of decrease was not very large. The average decreases for the three wave periods were 17.52%, 18.66%, and 4.53%, respectively. The heave motion obviously decreased with the increase in the draught, and the decrease became larger with the increase in the wave period. The average decreases during the three wave periods were 21.67%, 26.84%, and 29.83%, respectively. With regard to the surge motion, in two groups of waves with periods of 9 and 11 s, the surge motion of the platform decreased with the increase in diving depth. When the wave height was 10 m and the wave period was 11 s, the decrease was the largest, which was 59.5%. However, the surge motions of the platform under both normal and survival conditions were almost the same under the wave group with a
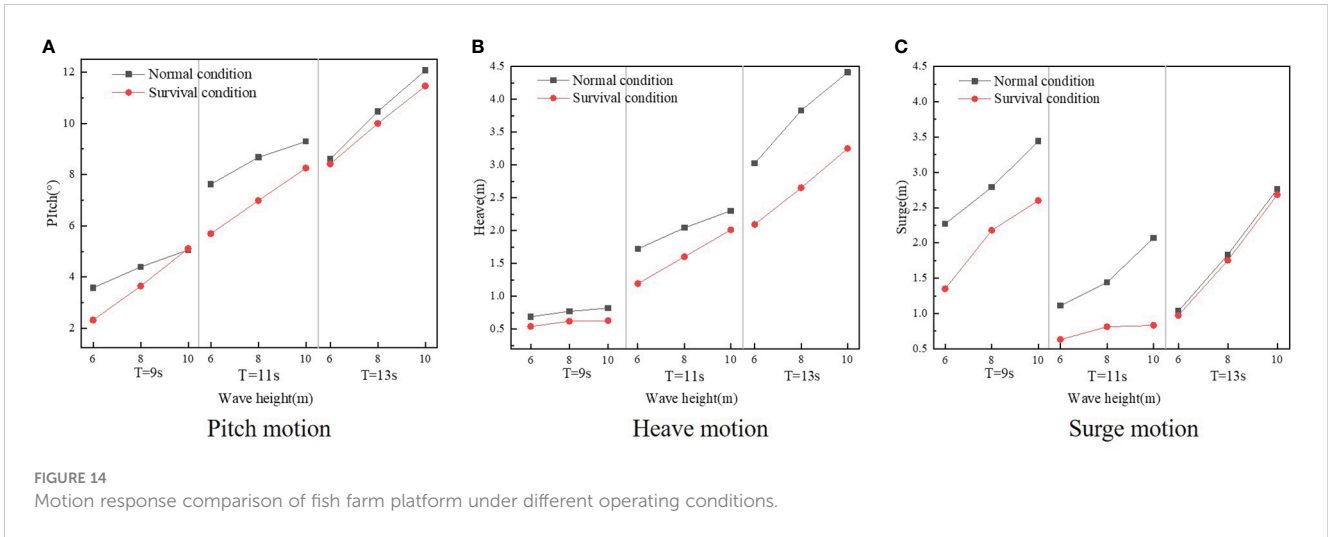

FIGURE 13
Motion response and mooring line tension of fish farm platform under different wave steepness.

FIGURE 14
Motion response comparison of fish farm platform under different operating conditions.

period of 13 s. These results indicate that the new fish farm platform can improve its seakeeping performance under extreme conditions by diving its main body through the water.

5.2 Mooring line tension

The mooring line tension of the fish farm platform under the survival condition was calculated and compared to that under the normal condition. The comparison results are shown in Figure 15. It was found that the mooring line tension of the fish farm platform under the survival condition had the same response law as the platform under the normal condition with changes in wave height and wave period. The mooring line tension was positively correlated with the wave height and negatively correlated with the wave period. In addition, under all wave conditions, the mooring line tension of the platform under the survival condition was less than that under the normal condition. This is mainly due to the impact of

the wave and current on the fish farm platform decreasing as the main structure of the platform dives into deeper water. In addition, it was found that the laid length increased with the increase of the draught of the platform, which reduced the initial mooring line tension. Furthermore, it should be noted that the decrease in mooring line tension between normal and survival conditions increased with the increase in wave height. This indicates that, in terms of mooring line tension, the new fish farm platform can deal with severe ocean conditions well by adjusting the draught of the platform.

6 Conclusion

In this study, a new semi-submersible vessel-shaped fish farm platform was developed. The hydrodynamic numerical model of the fish farm platform was established based on the AQWA software, and the corresponding physical model test was carried out to verify the numerical model. Based on the verified model, the hydrodynamic performance of the platform under different wave conditions was analyzed. The applicability of the platform to deal with extreme ocean conditions was studied from two aspects: motion response and mooring line tension. The conclusions drawn are as follows:

1) The motion response numerical simulation results agreed well with the physical model test results. The maximum error in mooring line tension was less than 5%. between the numerical and the physical model's test. The numerical model of the fish farm platform was fully verified, and the corresponding modeling method provided a reference for the establishment of a hydrodynamic model of a large truss fish farm platform.

2) There were correlations between pitch and heave motions. They were all positively correlated with wave height and wave period. The platform's mooring line tension was positively correlated with wave height and negatively correlated with wave period. In addition, surge motion
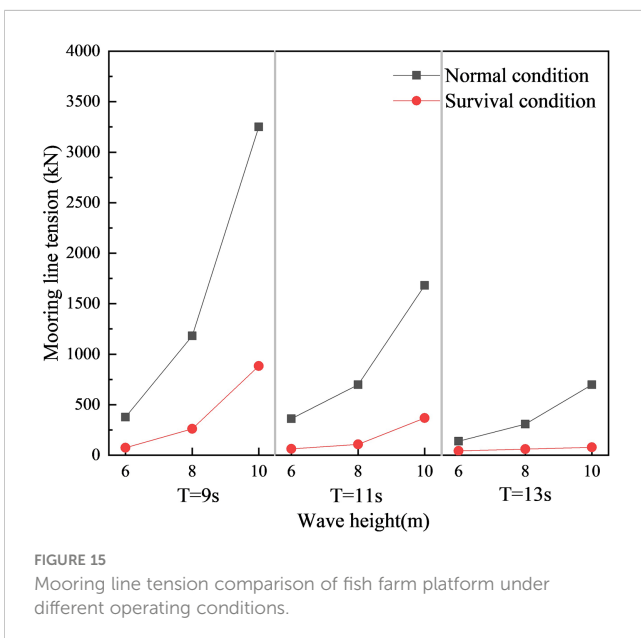

FIGURE 15
Mooring line tension comparison of fish farm platform under different operating conditions.

played an important role in the increase of mooring tension. Waves with large steepness values should be considered when designing a mooring system.

3) The new fish farm platform improved its seakeeping performance under extreme conditions by diving its main body through the water. The mooring line tension of the platform under the survival condition was much lower than that under the normal condition. This expressed the new semi-submersible vessel-shaped fish farm platform's ability to deal with extreme ocean conditions. The choice of a small waterplane area provided a reference for the design of a large fish farm platform.

Data availability statement

The original contributions presented in the study are included in the article/supplementary material. Further inquiries can be directed to the corresponding author.

Author contributions

All authors certify that they have participated sufficiently in the work to take public responsibility for the appropriateness of the experimental design and method, and the collection, analysis, and interpretation of the data. All authors contributed to the article and approved the submitted version.

Conflict of interest

The authors declare that the research was conducted in the absence of any commercial or financial relationships that could be construed as a potential conflict of interest.

Publisher's note

All claims expressed in this article are solely those of the authors and do not necessarily represent those of their affiliated organizations, or those of the publisher, the editors and the reviewers. Any product that may be evaluated in this article, or claim that may be made by its manufacturer, is not guaranteed or endorsed by the publisher.

References

ANSYS, AQWA (2018). *Aqwa theory manual* (Canonsburg, PA, USA: ANSYS, Inc).

Chu, Y. I., Wang, C. M., Park, J. C., and Lader, P. F. (2020). Review of cage and containment tank designs for offshore fish farming. *Aquaculture* 519, 734928. doi: 10.1016/j.aquaculture.2020.734928

Fredriksson, D. W., Decew, J. C., and Tsukrov, I. (2007). Development of structural modeling techniques for evaluating HDPE plastic net pens used in marine aquaculture. *Ocean Eng.* 34 (16), 2124–2137. doi: 10.1016/j.oceaneng.2007.04.007

Fredriksson, D. W., Swift, M. R., Irish, J. D., Tsukrov, I., and Celikkol, B. (2003). Fish cage and mooring system dynamics using physical and numerical models with field measurements. *Aquacultural Eng.* 27 (2), 117–146. doi: 10.1016/S0144-8609(02)00043-2

Gansel, L. C., Oppedal, F., Birkevold, J., and Tuene, S. A. (2018). Drag forces and deformation of aquaculture cages full-scale towing tests in the field. *Aquacultural Eng.* 81, 46–56. doi: 10.1016/j.aquaeng.2018.02.001

Huang, X. H., Guo, G. X., Tao, Q. Y., Liu, H. Y., Wang, S. M., and Hao, S. H. (2016). Numerical simulation of deformations and forces of a floating fish cage collar in waves. *Aquacultural Eng.* 74, 111–119. doi: 10.1016/j.aquaeng.2016.07.003

Huang, X. H., Guo, G. X., Tao, Q. Y., Liu, H. Y., Wang, S. M., and Hao, S. H. (2018). Dynamic deformation of the floating collar of a net cage under the combined effect of waves and current. *Aquacultural Eng.* 83, 47–56. doi: 10.1016/j.aquaeng.2018.08.002

Huang, X. H., Liu, H. Y., Hu, Y., Tao, Q. Y., Wang, S. M., and Liu, Z. X. (2020). Hydrodynamic performance of a semi-submersible offshore fish farm with a single point mooring system in pure waves and current. *Aquacultural Eng.* 90, 102075. doi: 10.1016/j.aquaeng.2020.102075

Kristiansen, T., and Faltinsen, O. M. (2012). Modelling of current loads on aquaculture net cages. *J. Fluids Structures* 34, 218–235. doi: 10.1016/j.jfluidstructs.2012.04.001

Kristiansen, T., and Faltinsen, O. M. (2015). Experimental and numerical study of an aquaculture net cage with floater in waves and current. *J. Fluids Structures* 54, 1–26. doi: 10.1016/j.jfluidstructs.2014.08.015

Lei, Y., Zhao, S. X., Zheng, X. Y., and Li, W. (2020). Effects of fish nets on the nonlinear dynamic performance of a floating offshore wind turbine integrated with a steel fish farming cage. *Int. J. Struct. Stability Dynamics* 20 (3), 2050042. doi: 10.1142/S021945542050042X

Lei, Y., Zheng, X. Y., Li, W., Zheng, H., Zhang, Q., Zhao, S., et al. (2021). Experimental study of the state-of-the-art offshore system integrating a floating offshore wind turbine with a steel fish farming cage. *Mar. structures* 80, 103076. doi: 10.1016/j.marstruc.2021.103076

Li, L., Jiang, Z., Hoilang, Av, and Ong, M. C. (2018a). Numerical analysis of a vessel-shaped offshore fish farm. *J. Offshore Mechanics Arctic Eng.* 140, 041201. doi: 10.1115/1.4039131

Li, L., Jiang, Z. Y., Ong, M. C., and Hu, W. F. (2019). Design optimization of mooring system: An application to a vessel-shaped offshore fish farm. *Eng. Structures* 197, 109363. doi: 10.1016/j.engstruct.2019.109363

Li, L., Jiang, Z., Wang, J. G., and Hu, W.F. (2018b) Numerical study on the heading misalignment and current velocity reduction of a vessel-shaped offshore fish farm. *J. Offshore Mechanics Arctic Eng.* 141, 051602. doi: 10.1115/1.4042266

Liu, H. F., Bi, C. W., Xu, Z., and Zhao, Y. P. (2021). Hydrodynamic assessment of a semi-submersible aquaculture platform in uniform fluid environment. *Ocean Eng.* 237, 109656. doi: 10.1016/j.oceaneng.2021.109656

Liu, H. F., Bi, C. W., and Zhao, Y. P. (2020). Experimental and numerical study of the hydrodynamic characteristics of a semisubmersible aquaculture facility in waves. *Ocean Eng.* 214, 107714. doi: 10.1016/j.oceaneng.2020.107714

Martin, T., Tsarau, A., and Bihs, H. (2020). A numerical framework for modelling the dynamics of open ocean aquaculture structures in viscous fluids. *Appl. Ocean Res.* 106, 102410. doi: 10.1016/j.apor.2020.102410

Rui, D. (2018). *Numerical modeling and analysis of a semi-submersible fish-cage* (Trondheim, Norway: Norwegian University of Science and Technology).

Wang, G., Martin, T., Huang, L., and Bihs, H. (2021). A numerical study of the hydrodynamics of an offshore fish farm using REEF3D. *J. Offshore Mechanics Arctic Eng.* 144, 021301. doi: 10.1115/1.4052865

Wang, G., Martin, T., Huang, L., and Bihs, H. (2022). Numerical investigation of the hydrodynamics of a submersible steel-frame offshore fish farm in regular waves using CFD. *Ocean Eng.* 254, 111362. doi: 10.1016/j.oceaneng.2022.111528

Wang, S., Shen, W., Guo, J., Yuan, T. P., Qiu, Y., Tao, Q. Y., et al. (2020). Engineering prediction of fatigue strength for copper alloy netting structure by

experimental method. *Aquacultural Eng.* 90, 102087. doi: 10.1016/j.aquaeng.2020.102087

Xu, Z., and Qin, H. (2020). Fluid-structure interactions of cage based aquaculture: From structures to organisms. *Ocean Eng.* 217, 107961. doi: 10.1016/j.oceaneng.2020.107961

Yu, Z., Amdahl, J., Kristiansen, D., and Bore, P. T. (2019). Numerical analysis of local and global responses of an offshore fish farm subjected to ship impacts. *Ocean Eng.* 194, 106653. doi: 10.1016/j.oceaneng.2019.106653

Zhao, Y. P., Guan, C. T., Bi, C. W., Bi, C. W., Liu, H. F., Cui, Y., et al. (2019). Experimental investigations on hydrodynamic responses of a semi-submersible offshore fish farm in waves. *J. Mar. Sci. Eng.* 7, 238. doi: 10.3390/jmse7070238

Zhao, Y. P., Li, Y. C., Dong, G. H., Gui, F. K., and Teng, B. (2007). A numerical study on dynamic properties of the gravity cage in combined wave-current flow. *Ocean Eng.* 34, 2350–2363. doi: 10.1016/j.oceaneng.2007.05.003